Eur J Nucl Med Mol Imaging (2010) 37:1935–1942
DOI 10.1007/s00259-010-1504-3

ORIGINAL ARTICLE

Activation of P-glycoprotein (Pgp)-mediated drug efflux by extracellular acidosis: in vivo imaging with ^{68}Ga-labelled PET tracer

Oliver Thews · Wolfgang Dillenburg · Marco Fellner · Hans-Georg Buchholz · Nicole Bausbacher · Mathias Schreckenberger · Frank Rösch

Received: 20 January 2010 / Accepted: 12 May 2010 / Published online: 4 June 2010

Abstract
Purpose In vitro it has been shown that the functional activity of P-glycoprotein (Pgp), an important drug transporter responsible for multidrug resistance, can be strongly increased by extracellular acidosis. Here mitogen-activated protein kinases (MAPK) (p38, ERK1/2) seem to play an important role for signal transduction. However, it is unclear whether these effects are also relevant in vivo.
Methods With the newly developed PET tracer Schiff base-based ^{68}Ga-MFL6.MZ the functional Pgp activity was visualized under acidic conditions and during inhibition of MAPKs non-invasively by means of microPET in rat tumours. Tumours were acidified either by inspiratory hypoxia (8% O_2) or by injection of lactic acid. Inhibitors of the MAPK were injected intratumourally.
Results With increasing tumour volume the tumour pH changed from 7.0 to 6.7 and simultaneously the Pgp activity increased almost linearly. When the tumour was acidified by direct lactic acid injection the PET tracer uptake was reduced by 20% indicating a higher transport rate out of the cells. Changing the inspiratory O_2 fraction to 8% dynamically led to a reduction of extracellular pH and in parallel to a decrease of tracer concentration. While inhibition of the p38 pathway reduced the Pgp transport rate, inhibition of ERK1/2 had practically no impact.
Conclusion An acidic extracellular environment significantly stimulates the Pgp activity. The p38 MAPK pathway plays an important role for Pgp regulation in vivo, whereas ERK1/2 is of minor importance. From these results new strategies for overcoming multidrug resistance (e.g. reducing tumour acidosis, inhibition of p38) may be developed.

Keywords P-glycoprotein · Acidosis · p38 · ERK1/2 · Transport activity · PET · ^{68}Ga · ^{68}Ga-MFL6.MZ

Abbreviations
Pgp P-glycoprotein

Introduction

Solid-growing tumours show several pronounced differences as compared to normal tissues with respect to morphological and histopathological features and also in terms of physiological characteristics at the cellular and tissue level. Due to an abnormally formed vascular network with blind endings, increased vascular permeability, loss of vascular hierarchy and impaired vasomotion [1, 2] insufficient tumour perfusion results [3]. As a consequence of the inadequate oxygen delivery, hypoxia or even anoxia is a commonly found feature of human and experimental

Part of this study forms the doctoral theses of W. Dillenburg and M. Fellner.

O. Thews (✉) · W. Dillenburg
Institute of Physiology and Pathophysiology,
University Medicine Mainz,
Duesbergweg 6,
55099 Mainz, Germany
e-mail: OLTHEWS@uni-mainz.de

M. Fellner · F. Rösch
Institute of Nuclear Chemistry, University of Mainz,
55099 Mainz, Germany

H.-G. Buchholz · N. Bausbacher · M. Schreckenberger
Department of Nuclear Medicine, University Medicine Mainz,
55101 Mainz, Germany

tumours [3, 4]. In order to ensure a sufficient energy supply for the tumour under hypoxic conditions, the cells force anaerobic metabolism resulting in an increased lactic acid formation [5] with pH even below 6.0 [3, 6] subsequently causing extracellular acidosis in the tumour tissue. On the other hand, numerous studies have demonstrated that the abnormal physiological microenvironment (e.g. hypoxia) in tumours may limit the efficacy of ionizing radiation [7, 8] but also may reduce the cytotoxicity of chemotherapeutic drugs [9, 10]. For the latter finding several mechanisms caused by the adverse metabolic environment (hypoxia, acidosis) have been discussed: (1) oxygen deficiency might directly influence the mechanism of action (pharmacodynamics) of antineoplastic drugs (e.g. alkylating agents) [11], (2) hypoxia can cause cell cycle arrest and in turn reduce the efficacy of agents acting only on proliferating cells [11, 12] and (3) hypoxia-induced extracellular acidosis may influence the intra-/extracellular distribution of drug [12, 13]. The third mechanism plays a role if the chemotherapeutic drug itself is a weak acid or base. Since these drugs can enter the cell through the lipid membrane primarily in their undissociated form, the extracellular pH directly influences the drug uptake. In an acidic environment for instance the uptake of weak bases is reduced. All of the above-described mechanisms of chemoresistance are caused by the specific metabolic parameters of tumours.

Besides this, reduced chemosensitivity may result from drug transporters which actively pump amphiphilic xenobiotics out of the cell [14, 15]. Modulation of these drug transporters (e.g. by inhibitors) can modify the cytotoxic efficacy of chemotherapy [16]. The best studied member of the so-called ABC transporter family is P-glycoprotein (Pgp) responsible for a multidrug-resistant phenotype of many human tumours. Besides constitutional differences in the Pgp expression of tumour entities or cell lines, the expression as well as the functional activity of the transporter have been shown to be regulated. Besides cytokines and growth factors, parameters of the metabolic microenvironment such as hypoxia, glucose depletion or reactive oxygen species have been shown to regulate both Pgp expression and function [17–20]. Recent studies [21–23] demonstrated in vitro that lowering the extracellular pH to 6.5 functionally increases the Pgp activity and by this reduces the cytotoxicity of those chemotherapeutic drugs which are a substrate of Pgp. This finding was not caused by an increased Pgp expression or a translocation of the pre-existing transporter to the outer cell membrane [22]. In vivo it has been shown that lowering the tumour pH by forcing anaerobic glycolysis decreases the cytotoxicity of daunorubicin [22] which could be attributed to acidosis-induced activation of Pgp. However, in these experiments the Pgp transport rate itself could not be measured in vivo. On the other hand, the results clearly revealed that mitogen-activated protein kinases (MAPK) (p38, ERK1/2) were responsible for the signalling pathway from the extracellular pH to an activation of Pgp [22]. Inhibition of p38 and ERK1/2 both reduced the Pgp activity in vitro and consequently increased the cytotoxicity of daunorubicin. Inhibition of only the p38 pathway led to higher apoptosis induction presumably by a reduced Pgp activity.

From these results, there is strong evidence that extracellular acidosis functionally increases the Pgp activity via a p38-mediated pathway in vivo [22]. However, with the techniques available a direct non-invasive measurement of the induced change of Pgp transport rate was not feasible in tumour-bearing animals. As recently a new tracer for PET imaging of the functional Pgp activity in vivo has been developed and evaluated [24], the hypothesis should be addressed whether it is possible to directly and quantitatively confirm that extracellular acidosis activates Pgp in solid tumours. In addition, it was another aim of this study to demonstrate in vivo with PET imaging that MAPKs play a key role for functional Pgp activation and by this for the development of multidrug resistance.

Materials and methods

Tumour and animal model

The subline AT1 of the rat Dunning R3327 prostate carcinoma was used in all experiments. This cell line functionally expresses Pgp [23]. Cells were grown in RPMI medium supplemented with 10% fetal calf serum (FCS) at 37°C under a humidified 5% CO_2 atmosphere and subcultivated once per week. For tumour implantation male Copenhagen rats (Charles River Wiga, Sulzfeld, Germany; body weight 150–200 g) housed in the animal care facility of the University of Mainz were used. Animals were allowed access to food and acidified water ad libitum before the investigation. All experiments had previously been approved by the regional Animal Ethics Committee and were conducted in accordance with the German Law for Animal Protection and the UK Co-ordinating Committee on Cancer Research (UKCCCR) Guidelines [25]. Solid carcinomas of the R3327-AT1 cell line were heterotopically induced by injection of AT1 cells (0.4 ml approximately 10^4 cells/μl) subcutaneously into the dorsum of the hind foot. Tumours grew as flat, spherical segments and replaced the subcutis and corium completely. Volumes were determined by measuring the three orthogonal diameters (d) of the tumours and using an ellipsoid approximation with the formula: $V = d_1 \times d_2 \times d_3 \times \pi/6$. Tumours were used when they reached a volume of between 1.0 and 2.0 ml approximately 10–14 days after tumour cell inoculation.

PET tracer

For imaging of the functional Pgp activity the tracer ^{68}Ga-MFL6.MZ was used as described earlier [24]. The complex consists of a hexadentate Schiff base that is labelled with the positron emitter ^{68}Ga ($T_{1/2}$=67.7 min, β^+ branching= 89%; Fig. 1). ^{68}Ga was eluted from a ^{68}Ge/^{68}Ga generator [26] with 10 ml HCl and online-immobilized on an acidic cation exchanger. Metal impurities were removed by a mixture of acetone and hydrochloric acid (1 ml; 80% acetone/0.15 M HCl). Subsequently, the ^{68}Ga was eluted from the cation exchanger by a second mixture of acetone and hydrochloric acid (0.4 ml; 97.6% acetone/0.05 M HCl). Labelling was performed with 20 µl of the ligand MFL6. MZ solution (1 mg/ml in EtOH, 30 nmol) in 400 µl 0.12 M HEPES sodium salt buffer at pH=4.3 by addition of the purified ^{68}Ga fraction at 75°C for 10 min. Radiochemical labelling yield and complex formation were determined by thin-layer chromatography (TLC) on silica and RP-18 plates with 90% methanol/10% isotonic saline on a Canberra Packard Instant Imager. For injection the tracer pH was adjusted to 7.4 with NaOH and diluted with isotonic saline.

The tracer itself is a substrate of Pgp and therefore is actively pumped out of the cell. For this reason the intratumoural concentration inversely reflects the activity of the drug transporter [24]. Besides the active efflux the intracellular concentration depends also on the tracer uptake. Since the compound is a weak acid the tracer influx is not hindered by the extracellular acidosis. In addition, since the tracer shows a relatively high lipophilicity [24], the uptake does not seem to be the limiting factor for the intracellular tracer concentration.

Animal PET studies

For microPET imaging, rats were anaesthetized with pentobarbital (40 mg/kg, intraperitoneal administration, Narcoren, Merial, Hallbergmoos, Germany). A catheter was inserted into the left jugular vein for radiotracer application and a tube was placed into the trachea.

The microPET imaging was performed on a microPET Focus 120 small animal PET (Siemens/Concorde, Knoxville, TN, USA). During PET measurements the animals were placed in the supine position and breathed room air spontaneously through the tracheal tube. After a 15-min transmission scan with an external ^{57}Co source, dynamic PET studies were acquired in 2-D mode. The radiotracer was administered as a bolus injection of 0.4–0.7 ml via the left jugular vein catheter. The mean injected activity of ^{68}Ga-MFL6.MZ was 44.0±1.5 MBq. Time-activity curves were obtained with varying time frames (1–5 min) for a total measuring interval of 60 min. The PET list-mode data were histogrammed into 14 frames and reconstructed using the ordered subset expectation maximization (OSEM) algorithm. Volumes of interest (VOIs) were defined for tumour and reference tissue (testis). The testis was used as a reference since it was in the field of view when imaging the tumours on the feet and because the tissue concentration was relatively constant between all animals on a low level indicating that the tracer is not taken up into this tissue. Ratios of tumour to reference tissue were calculated from an integral image between 10 and 60 min after tracer injection.

Intratumoural drug application

In order to acidify the extracellular tumour space, small amounts of lactic acid were injected directly intratumourally. Therefore, 50 µl of a 0.222 mM solution of lactic acid (in H_2O) was injected into the tumour tissue at a depth of 2–3 mm about 5–10 min prior to the tracer application. The same amount of a 0.222 mM sodium lactate solution was applied in the contralateral tumour and this tumour served as intra-individual control. For analysis, the tracer activity in acid treated tumours were normalized to that of the control tumours (=100%).

In order to study the signalling pathway responsible for pH-dependent activation of the Pgp transport activity, inhibitors of different MAPK pathways (p38, ERK1/2) were investigated, namely SB203580 and U0126 (Sigma-Aldrich, Steinheim, Germany) for inhibition of p38 and

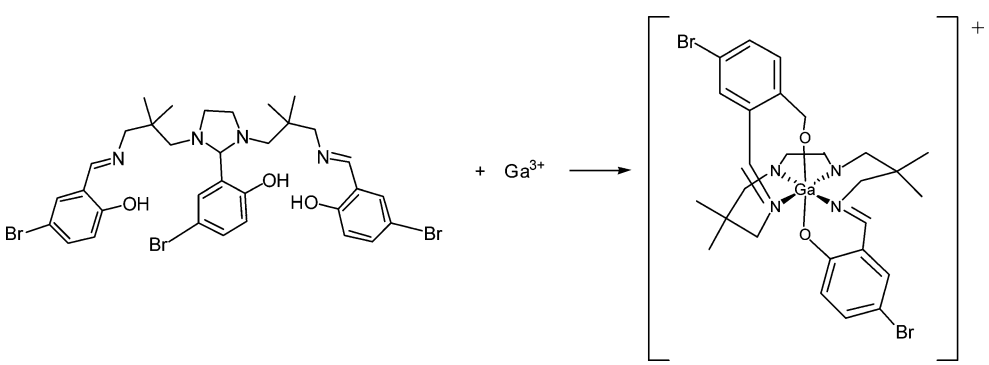

Fig. 1 MFL6.MZ used in the present study for complex formation with Ga^{3+} yielding ^{68}Ga-MFL6.MZ

ERK1/2, respectively. Since these inhibitors cannot be used systemically in animals, a direct intratumoural injection was chosen. Therefore, inhibitors were dissolved in dimethyl sulfoxide (DMSO) at a concentration of 1 mmol/l and tumours were treated with a single injection of these inhibitors 5–10 min prior to the PET measurements. This time point was used since previous experiments showed an effect of MAPK inhibitors in vivo definitely 30 min after injection [22] and since the analysis of tracer accumulation started 10 min after the onset of PET imaging. A small volume (20 µl) of the inhibitor stock solution was injected into the tumour resulting in a comparable tissue concentration as in previous cell culture experiments [22]. The tumour on the contralateral hind foot was treated with an injection of 20 µl DMSO only and served as intra-individual control. For further analysis the tracer uptake in the control tumours was set to be 100%.

Intratumoural pH measurement and inspiratory hypoxia

The extracellular pH was measured with steel-shafted pH glass electrodes (type MI-418B, Microelectrodes Inc., Bedford NH, USA) with an outer diameter of 800 µm. The electrode was inserted into the tumour and remained in place throughout the whole PET period. Before and after the PET imaging, the electrode was calibrated and pH measurements were corrected for signal shift.

In order to dynamically change the extracellular pH of the tumours, the inspiratory gas mixture was changed from pure oxygen (100% O_2) starting 10 min prior to the PET tracer injection to a hypoxic respiratory gas containing a mixture of 92% N_2+8% O_2 at 15 min after tracer injection (i.e. during the microPET measurement). It was continued until the end of the microPET measurement at 60 min. By reducing the inspiratory pO_2, glycolysis was forced in the tumour tissue leading to the formation of lactic acid. The change of extracellular pH was followed with the above-mentioned pH glass electrode which was placed in the centre of the tumour for the whole period of the microPET measurement.

Statistical analysis

Results are expressed as means ± SEM. Differences between groups were assessed by the two-tailed Wilcoxon test for paired samples. The significance level was set at α=5% for all comparisons. Correlation analysis was performed by calculating the Pearson correlation coefficient.

Results

The oxygenation worsens in AT1 tumours with increasing tumour volume [22]. As a result glycolysis is forced in larger tumours resulting in an increased formation of lactic acid and by this in a lowering of the extracellular pH with increasing tumour volume (at least in tumours below a volume of 1.9 ml; r=−0.941; Fig. 2a). In parallel, it was found that the tracer concentration in the tumour also tended to decrease with larger volume (Fig. 2b; r=−0.550, p=0.080). This reflects an increased Pgp activity in larger tumours as a result of a lower pH. Since pH measurements were not performed in the same tumours as Pgp PET imaging (to avoid the invasiveness of the pH measurement), the results shown in Fig. 2 are only a slight indication of the pH-dependent activation of Pgp.

Artificial acidification of the tumour

In order to acidify the tumour, a small amount (50 µl) of lactic acid (0.222 mM) was injected directly into the tumour to a depth of 2–3 mm. Since even this small volume might lead to pressure artefacts in the tissue, the contralateral tumour of each animal served as control. The direct comparison allows quantifying the effect of acidification solely on the tracer accumulation. Figure 3 shows an example of the tracer distribution in both tumours where the left tumour was treated with lactic acid. A region of reduced tracer accumulation can clearly be identified in the acid-treated tumour whereas in the contralateral control tumour (lactate) the ^{68}Ga-MFL6.MZ is homogeneously

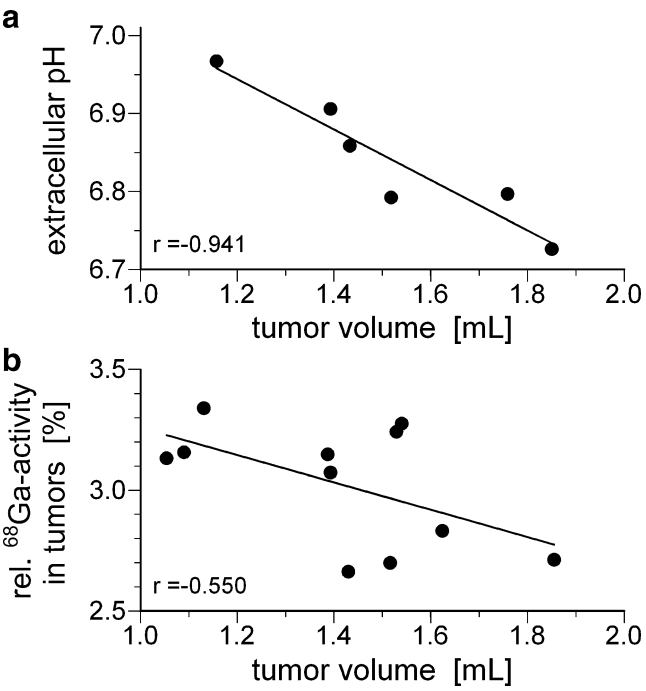

Fig. 2 Correlation of the extracellular pH (**a**) and the tracer accumulation (**b**) (normalized to the testis as reference tissue) with the tumour volume (r Pearson correlation coefficient)

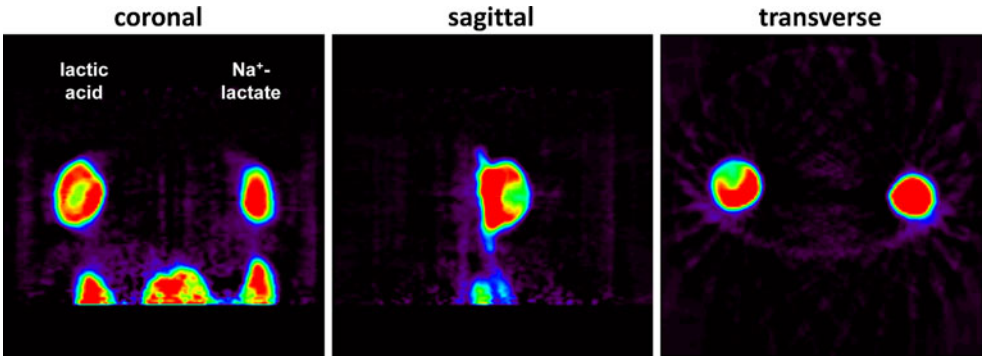

Fig. 3 Example of the tracer accumulation in subcutaneous tumours on the dorsum of the hind feet in different sectional plane microPET images. In the *left* tumour 50 µl of 0.222 mM lactic acid was injected whereas in the *right* tumour the same volume of an equimolar Na^+-lactate solution was applied

distributed. Since ^{68}Ga-MFL6.MZ is a substrate of Pgp, its decreased uptake in the tissue is the result of an increased Pgp activity. Figure 4 shows the statistical analysis of different animals in this experimental series. In most experiments the tracer concentration was markedly reduced in acidified tumours as compared to lactate-treated control tumours.

Figure 5 illustrates an example of an experiment where the pH was dynamically reduced during the imaging period by inspiratory hypoxia. The animal breathed 100% oxygen starting 10 min prior to the tracer injection. The online pH measurement showed a relatively stable pH of 6.95±0.01; 15 min after tracer injection the inspiratory O_2 fraction was reduced to only 8%, i.e. a value known to markedly affect the oxygenation of the tumour tissue [27]. Five minutes after the onset of inspiratory hypoxia, the intratumoural pH decreased to values around 6.8 (Fig. 5, triangles). With a slight delay the intratumoural tracer concentration decreased by 25–30% in both tumours.

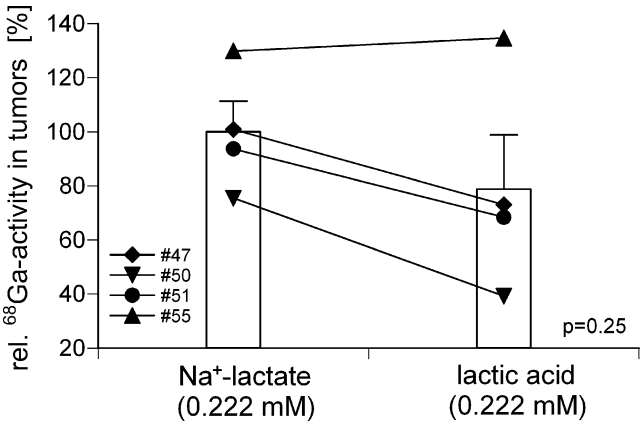

Fig. 4 Intratumoural relative ^{68}Ga-MFL6.MZ concentration (as defined by the activity ratio between tumour and testis) in tumours treated with lactic acid (50 µl, 0.222 mM) or with an equivalent volume of an equimolar Na^+-lactate solution. Each *line* represents one individual animal with two tumours on each hind foot. The activity values are normalized to the mean of the control tumour. *Columns* represent means ± SEM of all experiments

Inhibition of the MAPK pathways

A small volume (20 µl) of the inhibitor solution was injected into one tumour whereas the contralateral tumour served as control. Figure 6 illustrates an example where in the right tumour the p38 inhibitor SB203580 was injected whereas the left tumour only received DMSO. The right tumour shows a much higher tracer accumulation indicating a reduced Pgp activity. This effect was seen in all animals (Fig. 7) even though the comparison did not reach the level of statistical significance (p=0.06) as a result of the limited number of animals. On average, the SB203580-treated tumours showed a more than 70% higher tracer concentration than the contralateral control tumour. However, compared to completely untreated tumours, DMSO injection per se reduced the tracer accumulation markedly by approximately 50%. Compared to tumours without any

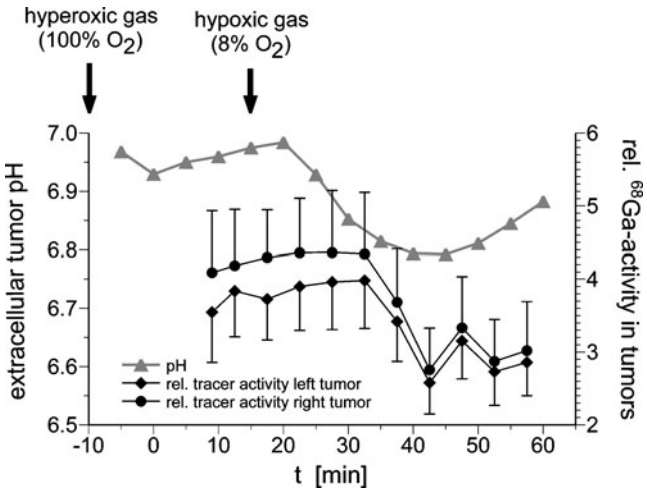

Fig. 5 Extracellular pH and ^{68}Ga-MFL6.MZ concentration ratio (tumour to testis) during change of the inspiratory O_2 fraction. The animal breathed 100% O_2 starting 10 min prior to tracer injection (t= 0 min); 15 min after tracer injection the respiratory gas mixture was changed to 8% O_2 and 92% N_2. The rapid circulatory redistribution of the tracer during the first 7 min has been omitted. The standard deviation of the tracer ratio describes the variability of the signal within the analysed VOI

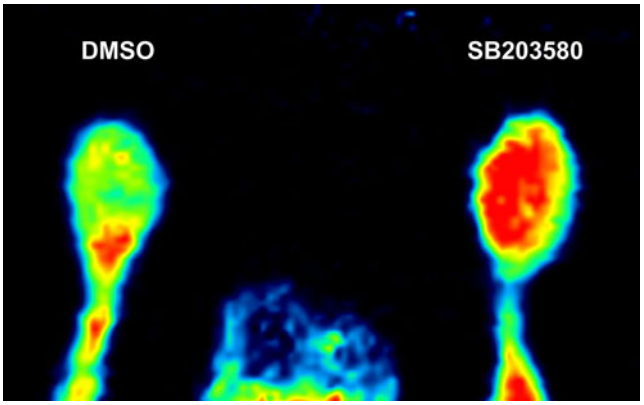

Fig. 6 Example of ^{68}Ga-MFL6.MZ accumulation in AT1 tumours. In the *right* tumour 20 µl of the p38 MAPK SB203580 inhibitor solution (1 mM in DMSO) was injected. The contralateral tumour received the same volume of DMSO alone

intratumoural injection, the tumour to testis tracer ratio in completely untreated tumours was 303±7%, whereas in DMSO-treated tumours it was 157±32%. These findings reveal that the direct intratumoural injection of the lipophilic solvent (DMSO) affects the tracer transport to the tumour cells. However, the direct comparison of SB203580 treatment with the DMSO-injected tumour in the same animal clearly proves that inhibition of the p38 signalling pathway reduces Pgp activity which is reflected by a higher ^{68}Ga-MFL6.MZ concentration.

Figure 8 shows the impact of inhibiting the ERK1/2 pathway by U0126. In U0126-treated tumours the PET tracer concentration was slightly higher than in DMSO-injected control tumours (p=0.25). On average, the tracer concentration was only 29% higher in the case of MAP inhibition. However, these results indicate that the ERK1/2 pathway plays a role in Pgp activation, although to a much lower extent.

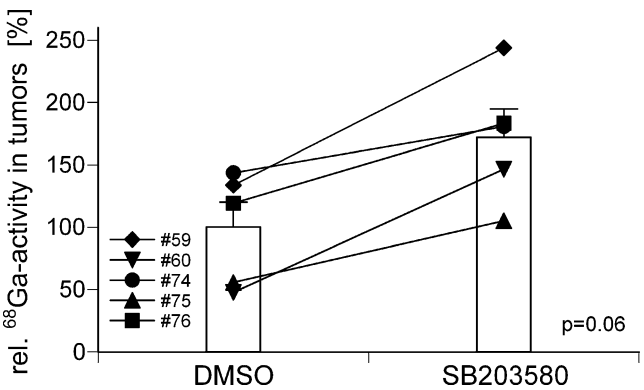

Fig. 7 Relative ^{68}Ga-MFL6.MZ concentration in tumours treated with the p38 MAPK inhibitor SB203580 (20 µl, 1 mM) or an equivalent volume of DMSO. Each *line* represents one individual animal with tumours on each hind foot. Values are normalized to the mean of the control tumour. *Columns* represent means ± SEM of all experiments

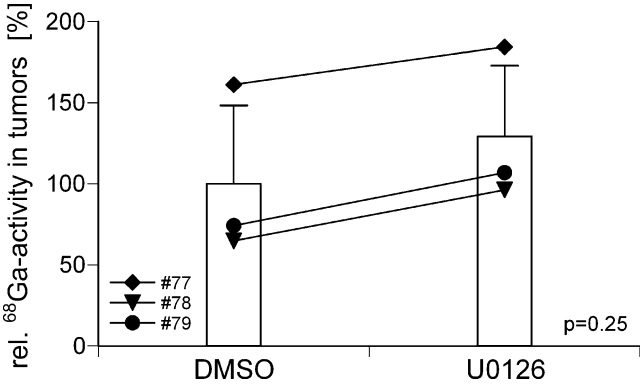

Fig. 8 Relative ^{68}Ga-MFL6.MZ concentration in tumours treated with the ERK1/2 MAPK inhibitor U0126 (20 µl, 1 mM) or an equivalent volume of DMSO. Each *line* represents one individual animal with tumours on each hind foot. Values are normalized to the mean of the control tumour. *Columns* represent means ± SEM of all experiments

Discussion

Pgp is the most important (and best studied) drug transporter of tumours which actively pumps chemotherapeutics out of the cells and therefore leads to a multidrug-resistant phenotype [28]. Recently, it could be demonstrated that a reduced extracellular pH was able to more than double the Pgp transport rate (but not the expression) [22, 23]. Since the in vivo measurement of changes of the transport rate was not possible in animal experiments, only a reduced chemosensitivity of tumours artificially made acidic (pH~6.5) has been described [22]. From parallels to the in vitro experiments it has been postulated that the reduced chemosensitivity was the result of a functional activation of Pgp. However, the final proof of this hypothesis is lacking [22].

With the development of a new ^{68}Ga-labelled PET tracer for imaging the functional transport rate it becomes possible to qualitatively measure the Pgp activity [24]. This tracer, ^{68}Ga-MFL6.MZ, was shown to be a substrate of Pgp. Therefore, its intratumoural concentration inversely mimics the Pgp-mediated transport. In the present study microPET images were analysed after acidifying the tumour tissue either by direct injection of lactic acid into the tumour or by forcing glycolytic metabolism. Since the interstitial fluid pressure is elevated in many human malignancies [29], the injection of even a small fluid volume such as 50 µl of lactic acid into the tissue may somehow (further) disturb tumour microcirculation. For this reason it cannot be excluded that the direct injection of the acid solution may reduce tumour perfusion locally and by this limit the tracer transport resulting in a locally reduced tracer accumulation. For this reason, the contralateral tumour of each animal served as an intra-individual control. In this tumour the same volume of an equimolar Na^+-lactate solution was injected probably leading to a comparable increase of the

interstitial hydrostatic pressure. The comparison of the tracer concentration in both tumours reflects therefore solely the impact of the lower pH on Pgp activity (Fig. 4).

The second method for acidifying the extracellular space was to force anaerobic glycolysis leading to an increased endogenous formation of lactic acid. Since oxygenation in experimental tumours worsens with increasing tumour size [22, 30], the formation of lactic acid will also be higher in larger tumours, which explains the even lower pH in larger tumours (at least in experimental tumour models) (Fig. 2a) [22]. In parallel to the reduced pH, the tracer concentration decreased with increasing tumour volume (Fig. 2b). This correlation can be interpreted as an increased Pgp activity in larger tumours as a result of increased hypoxia leading to a more pronounced acidosis. However, since the correlation is not strong, these findings are only a weak indication of an acidosis-induced activation of Pgp. The tracer uptake in larger tumours might also decrease if marked necrosis were to be found in these tumours. However, histological examination of AT1 tumours of this size did not show any necrosis (data not shown). For this reason necrosis formation as an explanation of reduced tracer uptake in larger tumours can probably be ruled out.

A more direct proof can be seen in the experiment in which during the microPET imaging the inspiratory gas mixture was reduced from pure oxygen to only 8% O_2 (Fig. 5). Several studies clearly demonstrated that inspiratory hypoxia worsens tumour oxygenation [27, 31] and by this leads to a reduced extracellular pH [22, 32]. In the present study hypoxia led to an increase in the Pgp activity resulting in a lower tracer accumulation as demonstrated by microPET imaging (Fig. 5). The reason why the pH starts rising again 30 min after the onset of the hypoxic breathing remains unclear at the moment. Maybe changes in the blood pressure or a hypoxia-induced vasodilation lead to an increase in tumour perfusion and by this to a better oxygen supply.

Previous in vitro data revealed that MAPKs (p38, ERK1/2) play a relevant role for signal transduction in the acidosis-induced activation of Pgp [22]. In vivo (in solid tumours) the increase in chemosensitivity after MAPK inhibition has been described [22]. The induction of apoptosis was increased after inhibiting the p38 pathway. Inhibition of ERK1/2 had almost no impact on the chemosensitivity. However, measuring cytotoxicity gives only indirect evidence that p38 affects the Pgp transport activity [22]. Therefore, the present study provides the first conclusive verification that the p38 signalling pathway is a relevant step from the extracellular pH to the activation of Pgp. Inhibition of p38 by SB203580 increased the intratumoural tracer concentration as a result of a higher Pgp activity (Fig. 7). As mentioned above a problem of the experimental design might be the direct intratumoural injection of drugs which might impair tumour perfusion. However, since in the contralateral tumour the same volume of DMSO alone was injected, the specific effect of SB203580 can be derived. In all tumours the activity in the SB203580-treated tumour was markedly higher (on average by a factor of 2) than in the control tumour even though the comparison did not reach the level of statistical significance (p=0.06; as a result of limited number of animals). Obviously, the inhibitor reduces the Pgp activity. Another problem might be the fact that DMSO has to be used as a solvent which may affect the tracer transport and uptake into the cell since the tracer is (at least partially) lipophilic [24]. Using the tumour to testis ratio as a measure of tracer accumulation, DMSO injection led to a markedly reduced intratumoural tracer level. In DMSO-treated tumours the ratio was 159±24%, whereas in untreated controls the ratio was 303±7%. These data indicate that DMSO injection per se reduces the tracer uptake which may be the result of pressure artefacts either by the injection or by a better solubility of the tracer in DMSO reducing its cellular uptake. However, independently of this finding the impact of SB203580 can be assessed from the comparison of the treated with the contralateral tumour. Inhibition of the p38 pathway seems therefore to be effective for reducing the Pgp transport rate.

The present findings on the impact of inhibition of ERK1/2 on the Pgp activity (Fig. 8) were comparable to those obtained on the daunorubicin toxicity [22]. In these previous experiments, ERK1/2 had practically no effect on chemosensitivity. In the present study ^{68}Ga-MFL6.MZ concentration was only increased by 29% after application of U0126. Therefore, the effect of p38 on Pgp activation seems to be much stronger than that of the ERK1/2 pathway.

In conclusion, the newly developed tracer ^{68}Ga-MFL6.MZ is a good choice to measure functional differences in the activity of Pgp. The present study clearly demonstrates that an acidic extracellular environment activates Pgp resulting in a strong drug efflux out of the cells. This mechanism might be one reason for the reduced chemosensitivity of hypoxic tumours. The results also prove that the p38 MAPK pathway plays an important role for Pgp regulation in vivo, whereas the impact of ERK1/2 is much less pronounced. With these experimental data in hand and the option of further systematic non-invasive imaging of Pgp-related effects in tumour treatment, new strategies for overcoming multidrug resistance may be developed either by reducing the extracellular acidosis or by inhibition of the p38 MAPK pathway. Using ^{68}Ga-MFL6.MZ and molecular imaging by means of PET/CT patients with chemoresistant tumours may be identified prior to therapy. On the other hand, PET imaging might be helpful in developing and evaluating new compounds (e.g. p38 inhibitors) for counteracting multidrug resistance.

Acknowledgments The study was supported by Deutsche Krebshilfe (grant 109136).

Conflicts of interest None.

References

1. Konerding MA, Malkusch W, Klapthor B, van Ackern C, Fait E, Hill SA, et al. Evidence for characteristic vascular patterns in solid tumours: quantitative studies using corrosion casts. Br J Cancer 1999;80:724–32.
2. Thews O, Kelleher DK, Vaupel P. Disparate responses of tumour vessels to angiotensin II: tumour volume-dependent effects on perfusion and oxygenation. Br J Cancer 2000;83:225–31.
3. Vaupel P, Kallinowski F, Okunieff P. Blood flow, oxygen and nutrient supply, and metabolic microenvironment of human tumors: a review. Cancer Res 1989;49:6449–65.
4. Höckel M, Vaupel P. Tumor hypoxia: definitions and current clinical, biologic, and molecular aspects. J Natl Cancer Inst 2001;93:266–76.
5. Mueller-Klieser W, Vaupel P, Streffer C. Energy status of malignant tumors in patients and experimental animals. In: Molls M, Vaupel P, editors. Blood perfusion and microenvironment of human tumors. Berlin: Springer; 1998. p. 193–207.
6. Stubbs M. Tumor pH. In: Molls M, Vaupel P, editors. Blood perfusion and microenvironment of human tumors. Berlin: Springer; 1998. p. 113–20.
7. Bush RS, Jenkin RD, Allt WE, Beale FA, Bean H, Dembo AJ, et al. Definitive evidence for hypoxic cells influencing cure in cancer therapy. Br J Cancer Suppl 1978;3:302–6.
8. Gray LH, Conger AD, Ebert M, Hornsey S, Scott OCA. The concentration of oxygen dissolved in tissues at the time of irradiation as a factor in radiotherapy. Br J Radiol 1953;26:638–48.
9. Sanna K, Rofstad EK. Hypoxia-induced resistance to doxorubicin and methotrexate in human melanoma cell lines in vitro. Int J Cancer 1994;58:258–62.
10. Teicher BA, Holden SA, Al-Achi A, Herman TS. Classification of antineoplastic treatments by their differential toxicity toward putative oxygenated and hypoxic tumor subpopulations in vivo in the FSaIIC murine fibrosarcoma. Cancer Res 1990;50:3339–44.
11. Teicher BA. Hypoxia and drug resistance. Cancer Metastasis Rev 1994;13:139–68.
12. Chaplin DJ, Horsman MR, Trotter MJ, Siemann DW. Therapeutic significance of microenvironmental factors. In: Molls M, Vaupel P, editors. Blood perfusion and microenvironment of human tumors. Berlin: Springer; 1998. p. 131–43.
13. Mahoney BP, Raghunand N, Baggett B, Gillies RJ. Tumor acidity, ion trapping and chemotherapeutics. I. Acid pH affects the distribution of chemotherapeutic agents in vitro. Biochem Pharmacol 2003;66:1207–18.
14. Higgins CF. ABC transporters: physiology, structure and mechanism—an overview. Res Microbiol 2001;152:205–10.
15. Schinkel AH, Jonker JW. Mammalian drug efflux transporters of the ATP binding cassette (ABC) family: an overview. Adv Drug Deliv Rev 2003;55:3–29.
16. Fojo T, Bates S. Strategies for reversing drug resistance. Oncogene 2003;22:7512–23.
17. Ledoux S, Yang R, Friedlander G, Laouari D. Glucose depletion enhances P-glycoprotein expression in hepatoma cells: role of endoplasmic reticulum stress response. Cancer Res 2003;63:7284–90.
18. Lee G, Piquette-Miller M. Cytokines alter the expression and activity of the multidrug resistance transporters in human hepatoma cell lines; analysis using RT-PCR and cDNA microarrays. J Pharm Sci 2003;92:2152–63.
19. Wartenberg M, Gronczynska S, Bekhite MM, Saric T, Niedermeier W, Hescheler J, et al. Regulation of the multidrug resistance transporter P-glycoprotein in multicellular prostate tumor spheroids by hyperthermia and reactive oxygen species. Int J Cancer 2005;113:229–40.
20. Yang JM, Sullivan GF, Hait WN. Regulation of the function of P-glycoprotein by epidermal growth factor through phospholipase C. Biochem Pharmacol 1997;53:1597–604.
21. Lotz C, Kelleher DK, Gassner B, Gekle M, Vaupel P, Thews O. Role of the tumor microenvironment in the activity and expression of the p-glycoprotein in human colon carcinoma cells. Oncol Rep 2007;17:239–44.
22. Sauvant C, Nowak M, Wirth C, Schneider B, Riemann A, Gekle M, et al. Acidosis induces multi-drug resistance in rat prostate cancer cells (AT1) in vitro and in vivo by increasing the activity of the p-glycoprotein via activation of p38. Int J Cancer 2008;123:2532–42.
23. Thews O, Gassner B, Kelleher DK, Schwerdt G, Gekle M. Impact of extracellular acidity on the activity of P-glycoprotein and the cytotoxicity of chemotherapeutic drugs. Neoplasia 2006;8:143–52.
24. Fellner M, Dillenburg W, Buchholz HG, Bausbacher N, Schreckenberger M, Rösch F et al. Radiopharmaceutical 68 Ga tracer for assessing p-glycoprotein (Pgp) activity in vivo. Mol Imaging Biol 2010; submitted.
25. Workman P, Twentyman P, Balkwill F, Balmain A, Chaplin DJ, Double JA, et al. United Kingdom Co-ordinating Committee on Cancer Research (UKCCCR) guidelines for the welfare of animals in experimental neoplasia (2nd edit.). Br J Cancer 1998;77:1–10.
26. Zhernosekov KP, Filosofov DV, Baum RP, Aschoff P, Bihl H, Razbash AA, et al. Processing of generator-produced 68Ga for medical application. J Nucl Med 2007;48:1741–8.
27. Thews O, Wolloscheck T, Dillenburg W, Kraus S, Kelleher DK, Konerding MA, et al. Microenvironmental adaptation of experimental tumours to chronic vs acute hypoxia. Br J Cancer 2004;91:1181–9.
28. Comerford KM, Wallace TJ, Karhausen J, Louis NA, Montalto MC, Colgan SP. Hypoxia-inducible factor-1-dependent regulation of the multidrug resistance (MDR1) gene. Cancer Res 2002;62:3387–94.
29. Fukumura D, Jain RK. Tumor microenvironment abnormalities: causes, consequences, and strategies to normalize. J Cell Biochem 2007;101:937–49.
30. Thews O, Kelleher DK, Lecher B, Vaupel P. Blood flow, oxygenation, metabolic and energetic status in different clonal subpopulations of a rat rhabdomyosarcoma. Int J Oncol 1998;13:205–11.
31. Kelleher DK, Thews O, Vaupel P. Hypoxyradiotherapy: lack of experimental evidence for a preferential radioprotective effect on normal versus tumor tissue as shown by direct oxygenation measurements in experimental sarcomas. Radiother Oncol 1997;45:191–7.
32. Kalliomäki T, Hill RP. Effects of tumour acidification with glucose+MIBG on the spontaneous metastatic potential of two murine cell lines. Br J Cancer 2004;90:1842–9.